

# Quantitative determination of delaminations in layered composites

Wolfgang Weigl and Eckart Schnack  
Institute of Solid Mechanics  
University of Karlsruhe, D-76128 Karlsruhe, Germany

## Abstract

In this contribution a new non-destructive determination method is presented for quantifying the size and location of delaminations on certain interfaces inside a layered composite from over-determined boundary data on the outer surface. The method is based on digital shearographic measurements of the surface deformation under a well-defined static load, providing the necessary input data for the solution of this inverse problem. Several numerical and experimental results with CFRP laminates under tension clearly confirm the good convergence and regularizing properties of our new method.

## 1. Introduction

Modern engineering materials like carbon-fibre reinforced plastic (CFRP) are often used in critical structural applications due to their favourable properties like high specific stiffness and strength. But their inherent anisotropy is also associated with specific failure modes like delaminations, i.e. debonding of adjacent layers, which endanger profoundly the remaining strength and stability of the structural part. The increasing usage of these materials in many industrial application fields leads to a rising need for fast and reliable non-destructive determination methods of such interfacial damage to ensure the safety and functionality of the components under investigation.

According to a Boeing study in [1] about 60% of all damages found during the inspection of composite parts in airplanes are delaminations which are typically caused by impact or critical loading. As has recently been shown by Gros et al. [2], shearography is most sensitive for the detection of low-energy impact damages in CFRP composites as compared to other NDT techniques like ultra-sonic, eddy-current or thermography. But the pure usage of shearography possesses only qualitative capabilities of damage detection, i.e. a first guess about the presence of internal damage and limited information about the internal

size only in simple cases [3]. Since especially the size and location of delaminations are decisive for the remaining strength of a component and the choice of suitable repair strategies, the non-destructive inspection of material seeking the *quantitative* determination of internal damages before and in service has gained increasing importance, e.g. in the aerospace industry.

It is our aim in this present paper to obtain a quantitative determination (i.e. size, shape and location) of the internal damaged interface areas from the measured deformation data on the outer surface by solving the corresponding inverse problem. In our approach this damage quantification is done by an approximate calculation of the displacement jump across the investigated interface(s) with our new reconstruction algorithm AICRA (see section 3).

## 2. Shearographic measurements

As input data for our new method shearographic measurements of the outer deformation state under a well-defined loading condition are used. The principle of our shearographic set-up is depicted in Figure 1, consisting of an illuminating part with a beam expander and the

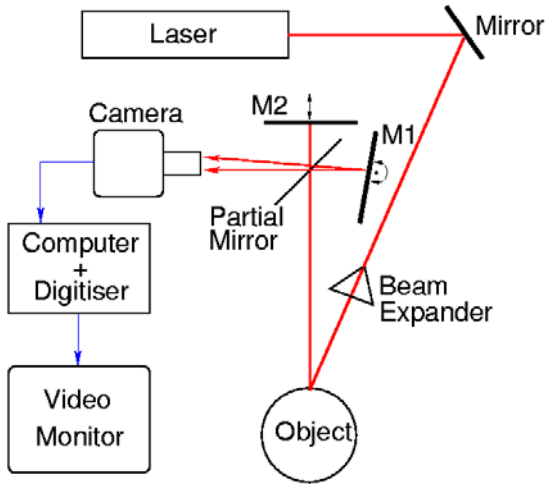


Figure 1: Digital shearography set-up

depicting part using a Michelson interferometer as shearing device. By slightly tilting the mirror M1 the shearing distance  $\Delta \mathbf{x}$  can be changed, whereas the mirror M2 is positioned on a piezo translator for applying the phase-shifting technique. With this method four intensity measurements are carried out in the unloaded and loaded object state, from which the relative phase difference  $\Delta \varphi$  is obtained pixel-wise,

with:

$$\Delta \varphi = \mathbf{k} \cdot [\mathbf{d}(\mathbf{x}) - \mathbf{d}(\mathbf{x} - \Delta \mathbf{x})], \quad (1)$$

$\mathbf{k}$  being the sensitivity vector and  $\mathbf{d}(\mathbf{x})$  the displacement vector in the surface point  $\mathbf{x}$ . After appropriate filtering, the resulting phase field images show clear black-white transitions, resolving even the direction of the phase gradient (see Figure 2a). After demodulation, these shearographic raw-data are further processed by a distinct integration to determine the corresponding displacement field  $\mathbf{d}(\mathbf{x})$  from the following summation [4]:

$$\sum_{j=0}^n \Delta\varphi(\xi - j\Delta\xi) = \mathbf{k} \cdot [\mathbf{d}(\mathbf{x}) - \mathbf{d}_0], \quad (2)$$

with an a priori known displacement vector  $\mathbf{d}_0 = \mathbf{d}(\mathbf{x} - (n+1)\Delta\mathbf{x})$  and  $\Delta\xi$  being the shearing distance in the image plane. The resulting displacement information (see Figure 2b) was

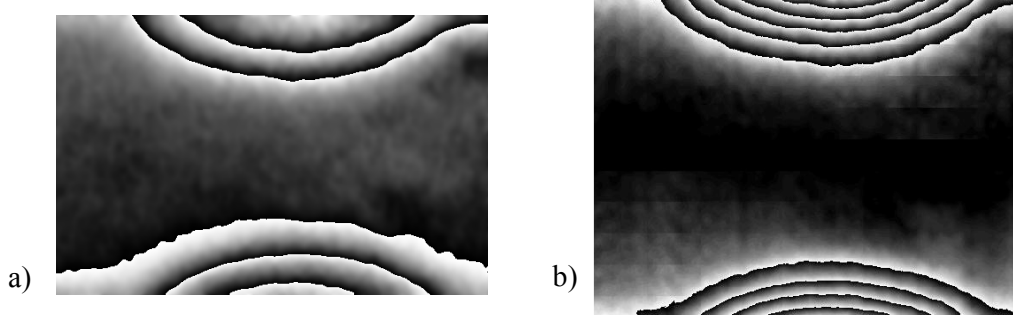


Figure 2: Out-of-plane measurements of a [+45-45,0,90]<sub>s</sub> CFRP laminate with boundary delaminations: a) filtered shearogram, b) calculated displacement field (pseudo ESPI)

shown to be in good agreement with three-dimensional FEM simulations. It is used as input data for our reconstruction algorithm, which will be described in Section 4.

### 3. Mathematical problem formulation

From a mathematical point of view, the determination of internal damage areas in layered CFRP material from over-determined boundary data on the outer surface can be described as follows:

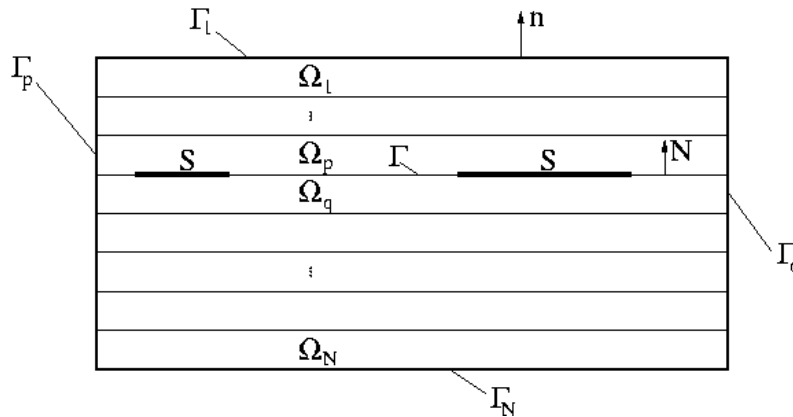


Figure 3: Delamination problem with a priori given interface  $\Gamma$

Consider a bounded domain  $\Omega \in \mathbb{R}^3$  consisting of  $N$  Lipschitz smooth subdomains  $\Omega_i$ , corresponding to the single layers of the laminate each having a different anisotropic material behaviour. The outer surface parts of the subdomain are denoted by  $\Gamma_i$ , whereas the inner interfaces between the domains  $\Omega_i$  and  $\Omega_j$  are called  $\Gamma_{ij}$  (see Figure 3). On the outer surface

$\partial\Omega = \bigcup_{i=1}^N \Gamma_i$ , both displacements  $\mathbf{u}^*$  and tractions  $\mathbf{t}^*$  are known due to measurements and

loading state. In a simplified approach, the delaminations  $S$  are assumed to lie on the a priori known interface  $\Gamma$ , between the two layers  $\Omega_p$  and  $\Omega_q$ . For the determination of the delaminations  $S$  the following elastostatic boundary value problem (bvp) is considered:

$$\begin{aligned}
\mathcal{A}_i \mathbf{u}_i &= \mathbf{0} && \text{in } \Omega_i, \\
\mathbf{u}_i &= \mathbf{u}^* && \text{on } \Gamma_i, \\
\mathcal{T}_i(\mathbf{n}) \mathbf{u}_i &= \mathbf{t}^* && \text{on } \Gamma_i, \\
\mathbf{u}_i - \mathbf{u}_j &= \mathbf{0} && \text{on } \Gamma_{ij} \setminus \Gamma, \\
\mathcal{T}_i(\mathbf{N}) \mathbf{u}_i - \mathcal{T}_j(\mathbf{N}) \mathbf{u}_j &= \mathbf{0} && \text{on } \Gamma_{ij} \setminus \Gamma, \\
\mathbf{u}_p - \mathbf{u}_q &= \mathbf{0} && \text{on } \Gamma \setminus S, \\
\mathcal{T}_p(\mathbf{N}) \mathbf{u}_p - \mathcal{T}_q(\mathbf{N}) \mathbf{u}_q &= \mathbf{0} && \text{on } \Gamma \setminus S, \\
\mathcal{T}_p(\mathbf{N}) \mathbf{u}_p = \mathcal{T}_q(\mathbf{N}) \mathbf{u}_q &= \mathbf{0} && \text{on } S,
\end{aligned} \tag{3}$$

where  $\mathbf{u}_i$  is the displacement solution,  $\mathcal{A}_i$  denotes the linear elasticity operator and  $\mathcal{T}_i$  the traction operator.

The basic idea of our approach is the quantitative determination of the damaged areas  $S$  by a reconstruction of the displacement jump across the investigated interface  $\Gamma$ . For this purpose, the outer loading conditions must be chosen in such a way that there is a normal opening of all possible delamination domains on  $\Gamma$ .

## 4. Reconstruction algorithm AICRA

The two-boundary variant of our new algorithm AICRA (Alternating Iterative Crack Reconstruction Algorithm) can be described as follows [5]:

- (1.) Choose an adapted start solution  $\mathbf{u}^{(0)}$  on  $\Gamma$ :
- (2.) Beginning with  $k=1$ , solve the two mixed bvps:

$$\begin{aligned}
\mathcal{A}_i \mathbf{u}_i^{(2k-1)} &= \mathbf{0} && \text{in } \Omega_i, \\
\mathbf{u}_i^{(2k-1)} - \mathbf{u}_j^{(2k-1)} &= \mathbf{0} && \text{on } \Gamma_{ij} \setminus \Gamma, \\
\mathcal{T}_i(\mathbf{N}) \mathbf{u}_i^{(2k-1)} - \mathcal{T}_j(\mathbf{N}) \mathbf{u}_j^{(2k-1)} &= \mathbf{0} && \text{on } \Gamma_{ij} \setminus \Gamma, \\
\mathbf{u}_p^{(2k-1)} &= \mathbf{u}_p^{(2k-2)} && \text{on } \Gamma, \\
\mathcal{T}_i(\mathbf{n}) \mathbf{u}_i^{(2k-1)} &= \mathbf{t}^* && \text{on } \Gamma_i,
\end{aligned} \tag{4}$$

with  $i \in \{1, \dots, p\}$  and

$$\begin{aligned}
\mathcal{A}_i \mathbf{u}_i^{(2k-1)} &= \mathbf{0} && \text{in } \Omega_i, \\
\mathbf{u}_i^{(2k-1)} - \mathbf{u}_j^{(2k-1)} &= \mathbf{0} && \text{on } \Gamma_{ij} \setminus \Gamma, \\
\mathcal{T}_i(\mathbf{N})\mathbf{u}_i^{(2k-1)} - \mathcal{T}_j(\mathbf{N})\mathbf{u}_j^{(2k-1)} &= \mathbf{0} && \text{on } \Gamma_{ij} \setminus \Gamma, \\
\mathbf{u}_q^{(2k-1)} &= \mathbf{u}_q^{(2k-2)} && \text{on } \Gamma, \\
\mathcal{T}_i(\mathbf{n})\mathbf{u}_i^{(2k-1)} &= \mathbf{t}^* && \text{on } \Gamma_i,
\end{aligned} \tag{5}$$

with  $i \in \{q, \dots, N\}$ , to obtain the solution  $\mathbf{u}_i^{(2k-1)}$ .

(3.) Solve the two mixed bvps:

$$\begin{aligned}
\mathcal{A}_i \mathbf{u}_i^{(2k)} &= \mathbf{0} && \text{in } \Omega_i, \\
\mathbf{u}_i^{(2k)} - \mathbf{u}_j^{(2k)} &= \mathbf{0} && \text{on } \Gamma_{ij} \setminus \Gamma, \\
\mathcal{T}_i(\mathbf{N})\mathbf{u}_i^{(2k)} - \mathcal{T}_j(\mathbf{N})\mathbf{u}_j^{(2k)} &= \mathbf{0} && \text{on } \Gamma_{ij} \setminus \Gamma, \\
\mathbf{u}_i^{(2k)} &= \mathbf{u}^* && \text{on } \Gamma_i, \\
\mathcal{T}_p(\mathbf{N})\mathbf{u}_p^{(2k)} &= \mathbf{t}_p^{(2k-1)} && \text{on } \Gamma,
\end{aligned} \tag{6}$$

with  $i \in \{1, \dots, p\}$  and

$$\begin{aligned}
\mathcal{A}_i \mathbf{u}_i^{(2k)} &= \mathbf{0} && \text{in } \Omega_i, \\
\mathbf{u}_i^{(2k)} - \mathbf{u}_j^{(2k)} &= \mathbf{0} && \text{on } \Gamma_{ij} \setminus \Gamma, \\
\mathcal{T}_i(\mathbf{N})\mathbf{u}_i^{(2k)} - \mathcal{T}_j(\mathbf{N})\mathbf{u}_j^{(2k)} &= \mathbf{0} && \text{on } \Gamma_{ij} \setminus \Gamma, \\
\mathbf{u}_i^{(2k)} &= \mathbf{u}^* && \text{on } \Gamma_i, \\
\mathcal{T}_q(\mathbf{N})\mathbf{u}_q^{(2k)} &= \mathbf{t}_q^{(2k-1)} && \text{on } \Gamma,
\end{aligned} \tag{7}$$

with  $i \in \{q, \dots, N\}$  to obtain the solution  $\mathbf{u}_i^{(2k)}$ .

(4.) Calculate the approximate jump of the displacement across the interface  $\Gamma$  by using the last approximations  $\mathbf{u}_i^{(2k)}$ :

$$[\mathbf{u}]^{(2k)}|_{\Gamma} = \mathbf{u}_p^{(2k)}|_{\Gamma} - \mathbf{u}_q^{(2k)}|_{\Gamma} \tag{8}$$

(5.) Define the approximate delamination domains  $S_\varepsilon^{(2k)}$  by introducing a small parameter  $\varepsilon^{(2k)}$  and setting

$$S_\varepsilon^{(2k)} = \left\{ \mathbf{x} \in \Gamma : [\mathbf{u}^{(2k)}(\mathbf{x})] \cdot \mathbf{N} > \varepsilon^{(2k)} \right\}. \tag{9}$$

(6.) Repeat the steps (2.) to (5.) until a given stopping criterion is fulfilled:

In contrast to the often used optimization approaches, no a priori assumptions on the number and shape of the delaminations are needed with AICRA. As further advantages, the algorithm provides good convergence and regularizing properties as well as a wide

applicability for related problems, e.g. glue contacts or electrostatic investigations. Besides, in the so-called three-boundary variant, the knowledge of the complete Cauchy data ( $\mathbf{u}^*$ ,  $\mathbf{t}^*$ ) is only needed on some part of the whole outer boundary [5].

## 5. Results and discussion

Several numerical and experimental tests were carried out to test our new algorithm. Special CFRP samples of the dimension  $200 \times 20 \times 4.4 \text{ mm}^3$  were used, where semi-elliptic interfacial

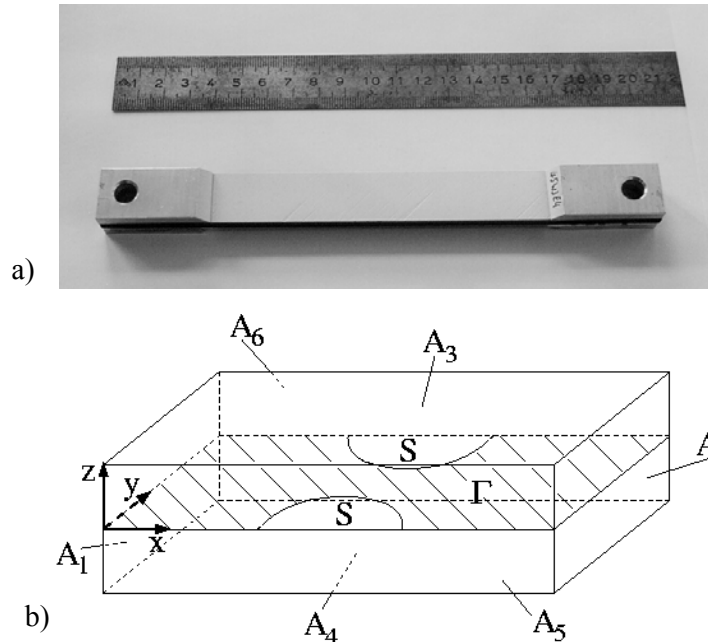


Figure 5: a) CFRP tension sample with predefined delamination  
b) Geometrical representation of this sample in FEM

damage areas had been predefined by incorporating Teflon foil. At both ends of the samples aluminium bars were agglutinated for applying the uniaxial tension load (see Figure 5a). The chosen prepreg FIBREDUX 913C from HEXCEL COMPOSITES is also used in current Airbus airplanes.

The numerical calculation of the internal displacement jump with the algorithm AICRA as

described above was implemented with three-dimensional FEM using ANSYS 5.6. In the two-boundary variant, it was assumed that the complete Cauchy data ( $\mathbf{u}^*$ ,  $\mathbf{t}^*$ ) were known on the whole outer boundary ( $A_1$  to  $A_6$  in Figure 5b). However, in the three-boundary variant, only on the side surfaces  $A_1$  to  $A_4$  full Cauchy data was given, whereas on  $A_5$  and  $A_6$  merely the traction free state (i.e.  $\mathbf{t}^* = \mathbf{0}$ ) was taken as boundary condition. Experimental shearographic results were used as input data  $\mathbf{u}^*$  as well as numerical data from FEM simulations of the corresponding direct problem. In the later case, an additional amount of 5% artificial noise was applied to the numerical boundary data by appropriately scaled random digits for simulating the inevitable measurement errors.

In Figure 6 the reconstruction results for the normal displacement jump  $[u_N]$  in the middle interface  $\Gamma$  are depicted for a symmetric CFRP sample with the stacking sequence

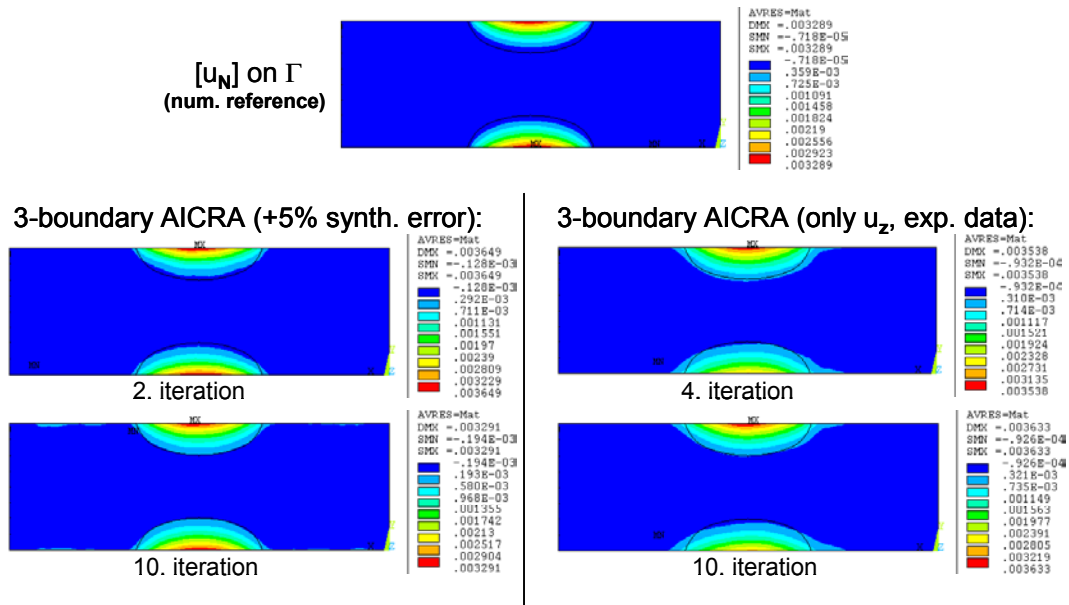


Figure 6: Reconstruction of the normal displacement jump  $[u_N]$  on  $\Gamma$  in  $[+45,-45,0,90]_s$  CFRP samples: top: numerical reference solution; left: numerical boundary data (+5% noise); right: shearographic data  $[+45,-45,0,90]_s$ . At the top of Figure 6, the sought reference solution is shown, which was obtained by numerically solving the direct problem with the predefined correct size of the internal delamination using FEM. As can clearly be seen, the approximated results using AICRA coincide well with the numerical reference solution, already after very few iterations. This is valid both for the numerical boundary data (Figure 6, left) as well as for the experimental displacement data using the digital phase-shifting shearography as described in section 2 (see Figure 6, right). The correct shape, size and location of the two semi-elliptical delaminations (as indicated by the black lines) can directly be obtained from the colour images of the normal displacement jump in Figure 6.

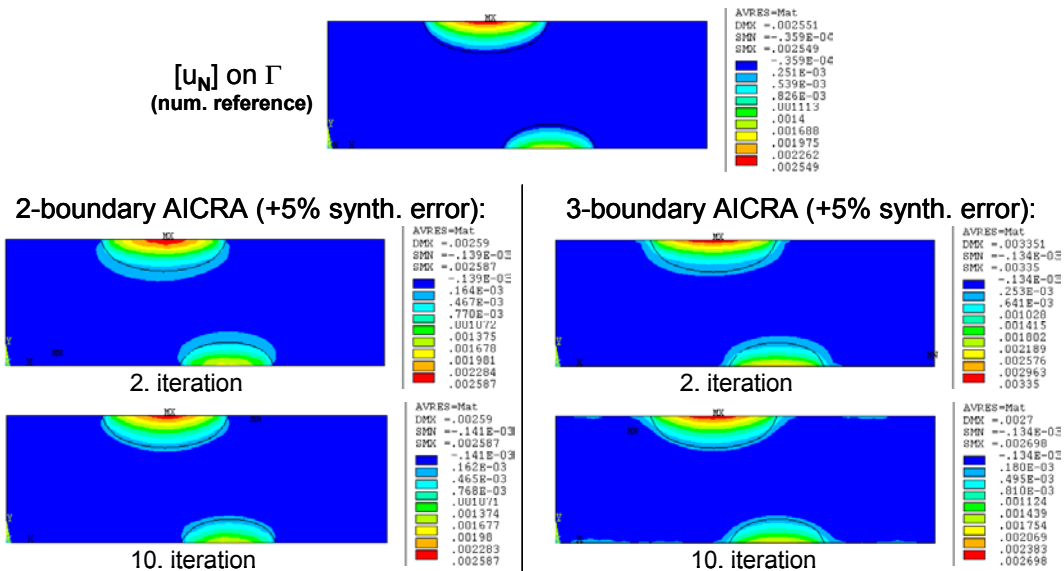


Figure 7: Reconstruction of  $[u_N]$  on  $\Gamma$  in  $[+45,-45,0,90,0,-30+30]$  CFRP samples: top: numerical reference solution; left: numerical data (+5% noise); right: numerical data (+5% noise)

In Figure 7 reconstruction results for the normal displacement jump  $[u_N]$  in the middle interface  $\Gamma$  are depicted for a non-symmetric CFRP sample with doubled thickness (8.8mm) and stacking sequence  $[+45,-45,0,90,90,0,-30,+30]$ . Now, the results of the two-boundary variant of AICRA are compared with the three-boundary variant, both using numerical boundary data with 5% of additional artificial noise. Again, the semi-elliptic internal damage domains can easily be obtained from the approximated displacement jump already after very few iterations of AICRA.

Finally, it can be concluded that the results on our CFRP tension samples clearly demonstrate the good and fast damage quantification properties of both variants of AICRA under real experimental conditions, offering a promising basis for further investigations on industrial composite parts.

#### **Literature:**

- [1] Miller AG, Lovell, DT and Seferis JC 1994: The evolution of an aerospace material: Influence of design, manufacturing and in-service performance. *Composite Structures* **27**, pp. 193-206.
- [2] Gros XE, Takahashi K and De Smet M-A 1999: On the efficiency of current NDT methods for impact damage detection and quantification in thermoplastic toughened CFRP material, *NDT.net* **4**(3).
- [3] Weikl W, Findeis D, Schnack E and Gryzagoridis J 2000: Comparing optical interference techniques for the non destructive detection of delaminations in layered composites, *Proceedings of The Seventh Annual International Conference on Composites Engineering, ICCE7, Denver CO, 2000*, pp. 921-922.
- [4] Waldner S 1996: Removing the image-doubling in shearography by reconstruction of the displacement field, *Optics Communications* **127**, pp. 117-126.
- [5] Weikl W, Andrä H and Schnack E 2001: An alternating iterative algorithm for the reconstruction of internal cracks in a three-dimensional solid body, *Inverse Problems* **17**(6), pp. 1957-1975.